Electronic Supplementary Material (ESI) for Journal of Materials Chemistry C.

Electronic Supporting Information

Vacuum deposition of high-quality thin films displaying spin transition near room temperature

Victoria Shalabaeva, Sylvain Rat, Maria Dolores Manrique-Juarez, Alin-Ciprian Bas, Laure Vendier, Lionel Salmon, Gábor Molnár* and Azzedine Bousseksou*

LCC, CNRS and Université de Toulouse, UPS, INP, F-31077 Toulouse, France

*Corresponding authors: gabor.molnar@lcc-toulouse.fr, azzedine.bousseksou@lcc-toulouse.fr; Fax: +33 05 61 55 30 03; Tel: +33 05 61 33 31 90

Figure S1. AFM topography images of a pristine thermally evaporated film (75 nm thickness). Image sizes are 10 × 10 μm^2.

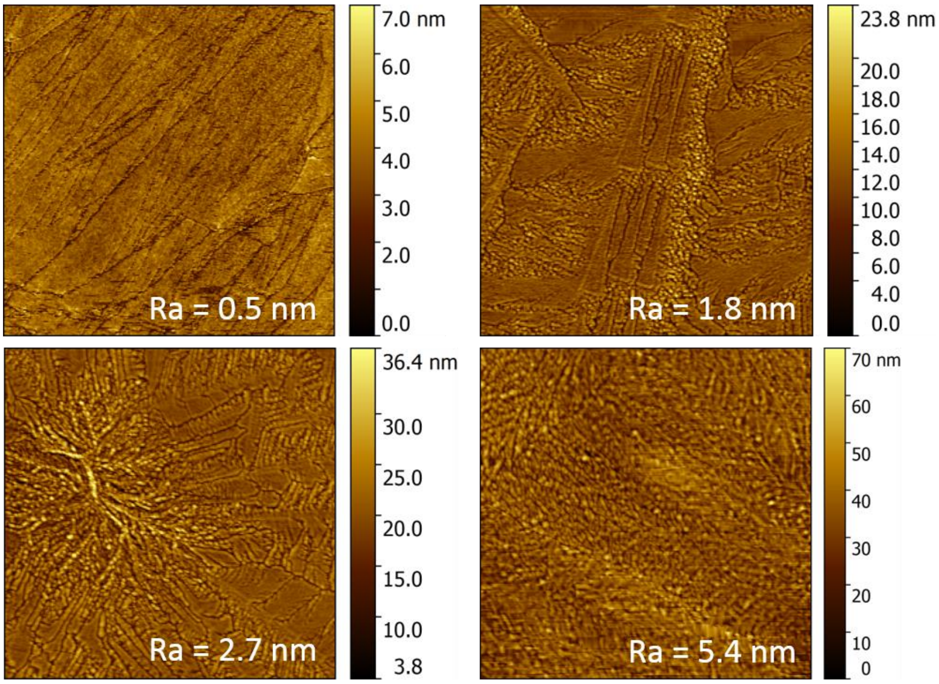

Figure S2. UV-Vis absorbance spectra of a 90 nm crystalline film at 293 K (LS) and 393 K (HS) deposited on a fused silica substrate. Inset: zoom on the visible spectral range.

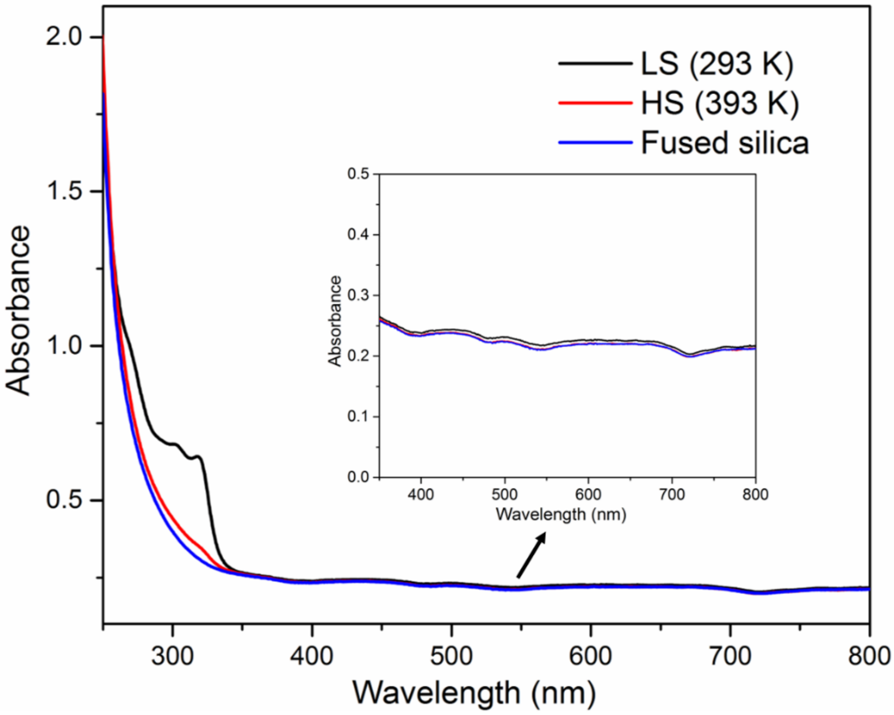

Figure S3. XRD patterns of pristine films with different thicknesses and storage times.

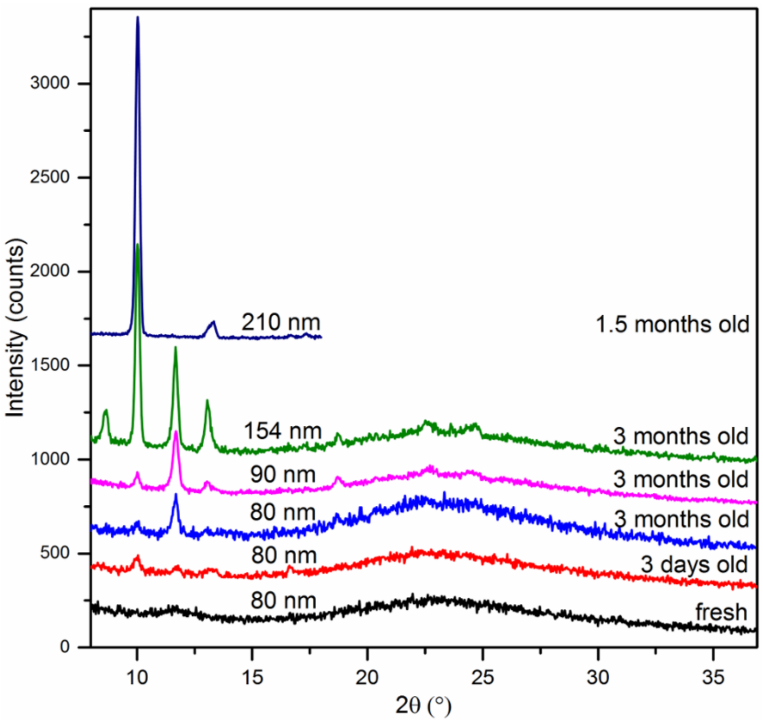

Figure S4. Film annealing at high-temperature. Optical images of films annealed at 160°C (a) and 220°C (b). AFM images of films annealed at 160°C (c) and 220°C (d). UV-Vis absorbance spectra of annealed films (at 160, 220 and 280 °C) and humidity treated films (e).

Freshly evaporated films were annealed at three different temperatures 160, 220 and 280 °C for 15 s on a hot plate. Annealing at 280°C led to a complete film destruction. Films annealed at 160°C showed inhomogeneous morphology as evidenced by optical imaging. Films annealed at 220°C show better crystallinity, but also a heterogeneous structure on the whole surface of the sample with significant roughness (R_a = 29 nm) and they become hazy when observed by naked eye. Compared to humidity treated films, in the UV-Vis spectra of annealed films the absorbance values are not proportional to the film thickness and the baseline tends to increase due to light scattering.

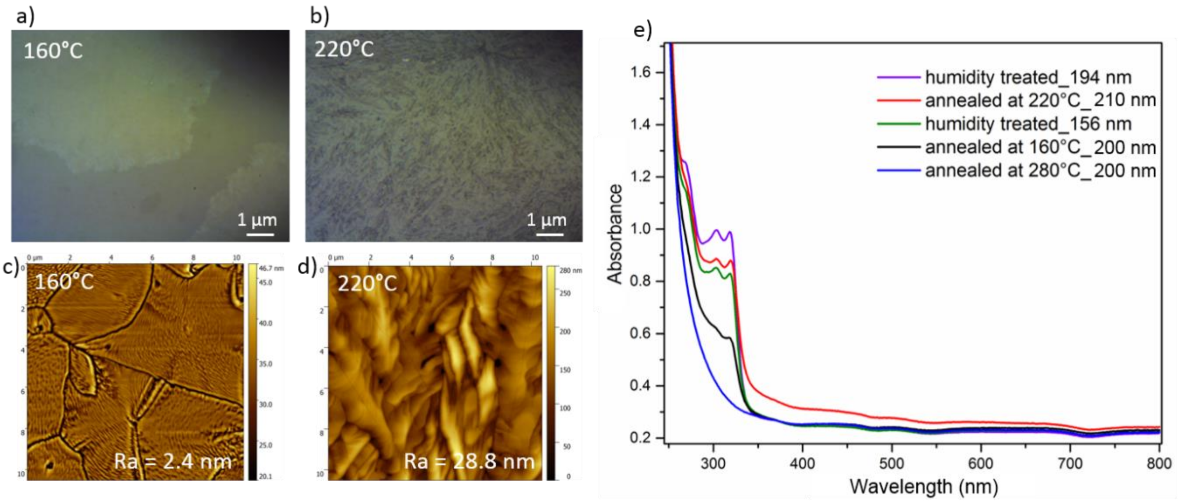

Figure S5. Selected AFM images of crystalline films obtained by solvent vapour annealing: (a)-(b) two different zones of 90 nm film; (c) 90 nm film after 3 months of storage in ambient air; (d) 150 nm film with roughness 2.5 nm; (e) film thickness evaluation.

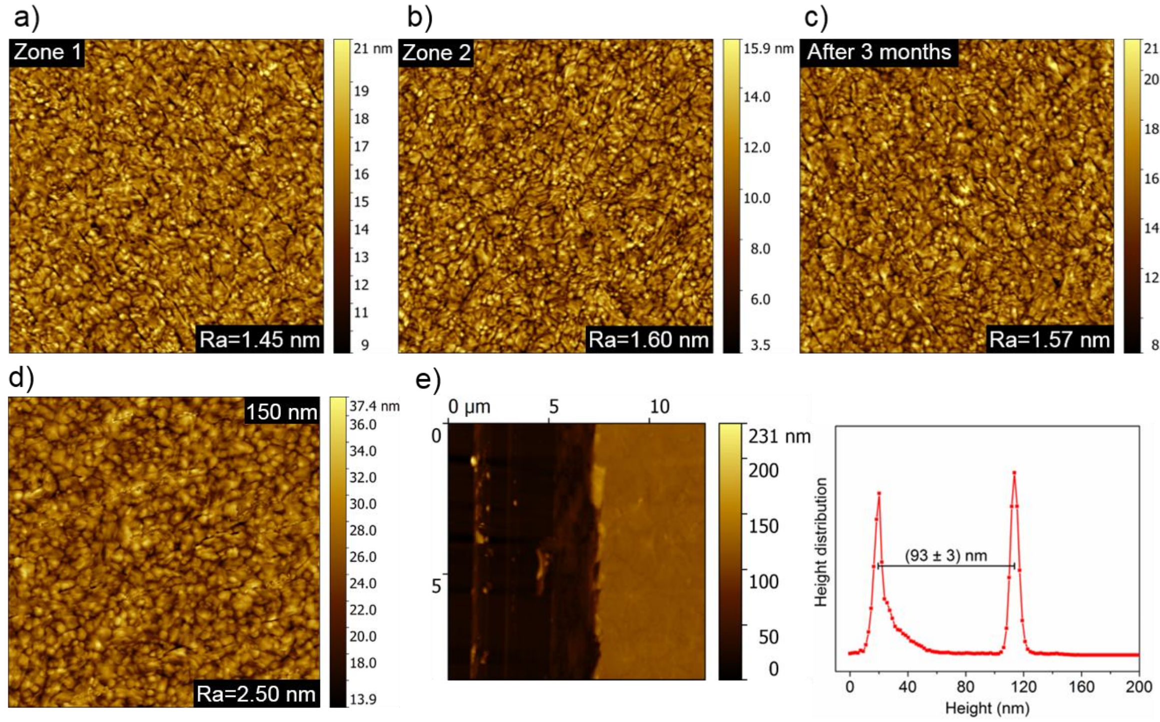

Figure S6. Evaluation of the degree of crystallinity and the completeness of the spin transition in the films. The graph shows the variation in absorbance between the LS and HS states (Abs_{LS}-Abs_{HS}) for various film thicknesses. The black squares correspond to the experimentally measured values, while the red line corresponds to the theoretically expected values for a fully complete spin transition. This evaluation is based on the assumption that the 194 nm film displays a complete spin transition, which was inferred from the temperature dependent Raman analysis of this film (see Fig. 7 in the main text).

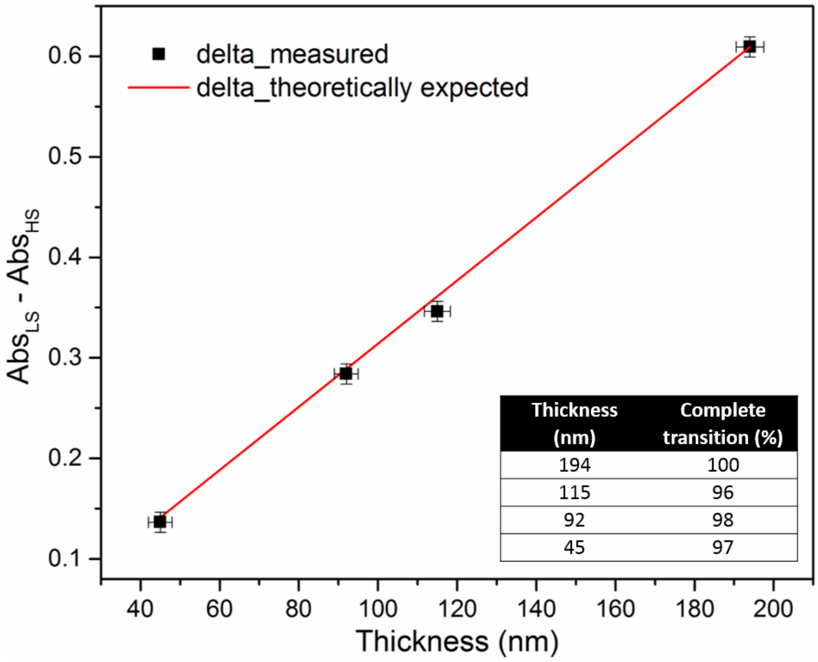

Thickness (nm)	Complete transition (%)
194	100
115	96
92	98
45	97

Figure S7. PXRD patterns of the bulk powder at low and high spin. The peak corresponding to the (002) reflection shifts from 2θ = 10.11° at 303 K to 9.59° at 373 K.

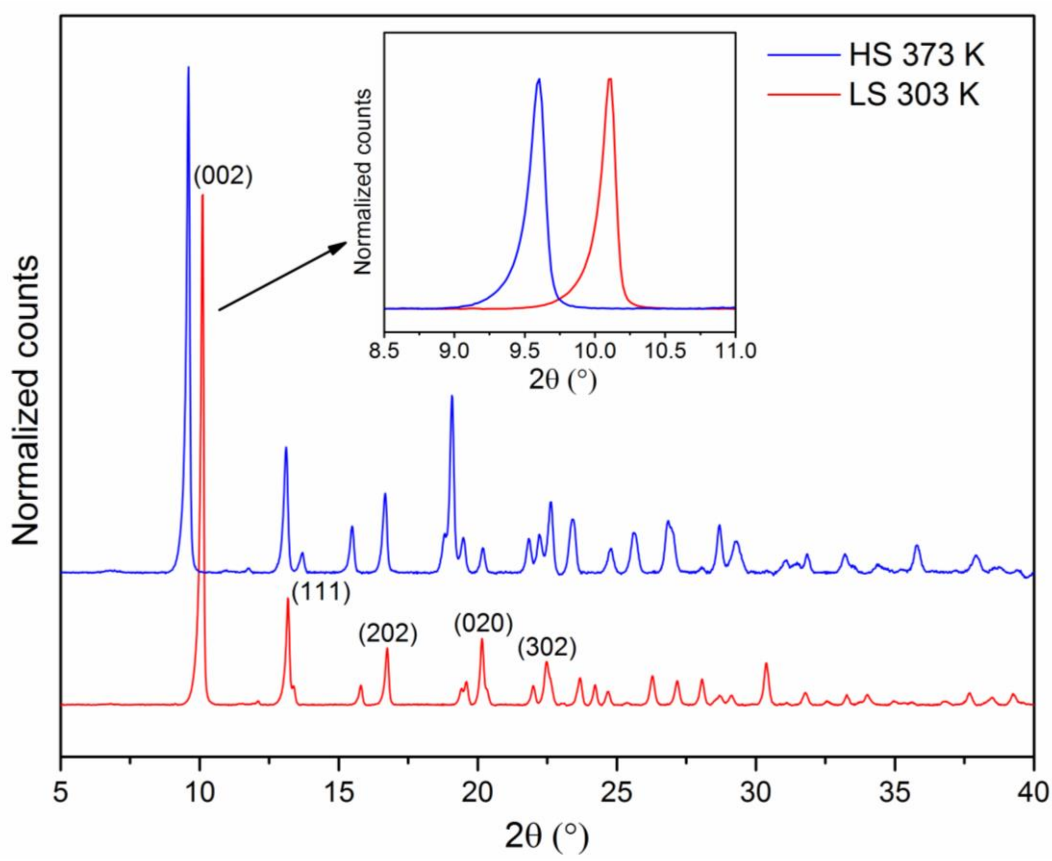

Figure S8. XRD patterns of a 194 nm crystalline film at different temperatures.

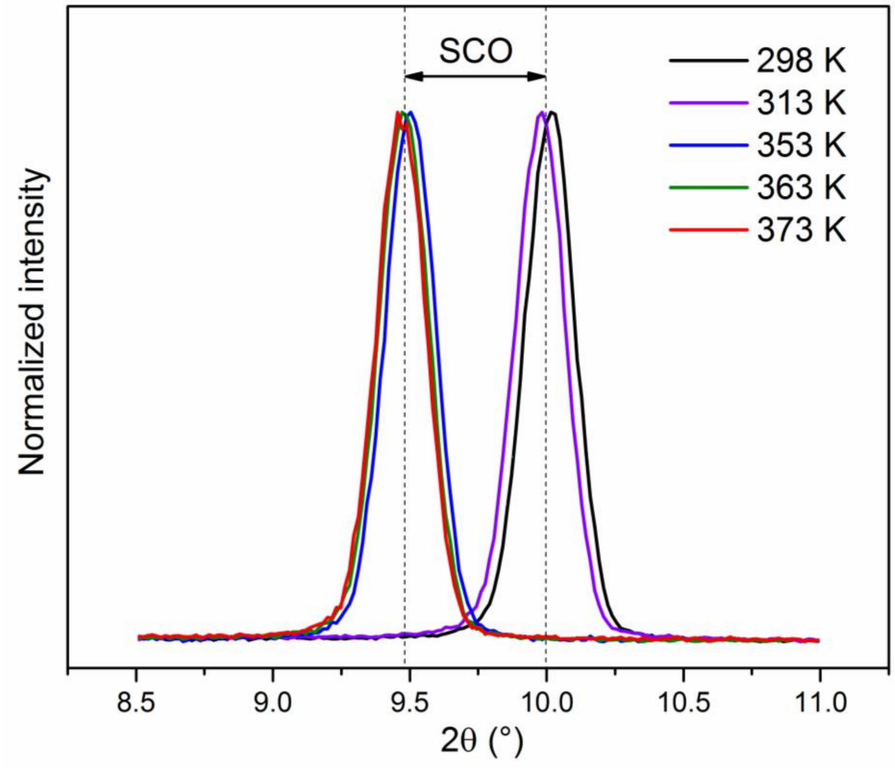

Figure S9. XRD patterns of solvent annealed films on different substrates (fused silica, single crystalline silicon and polycrystalline gold).

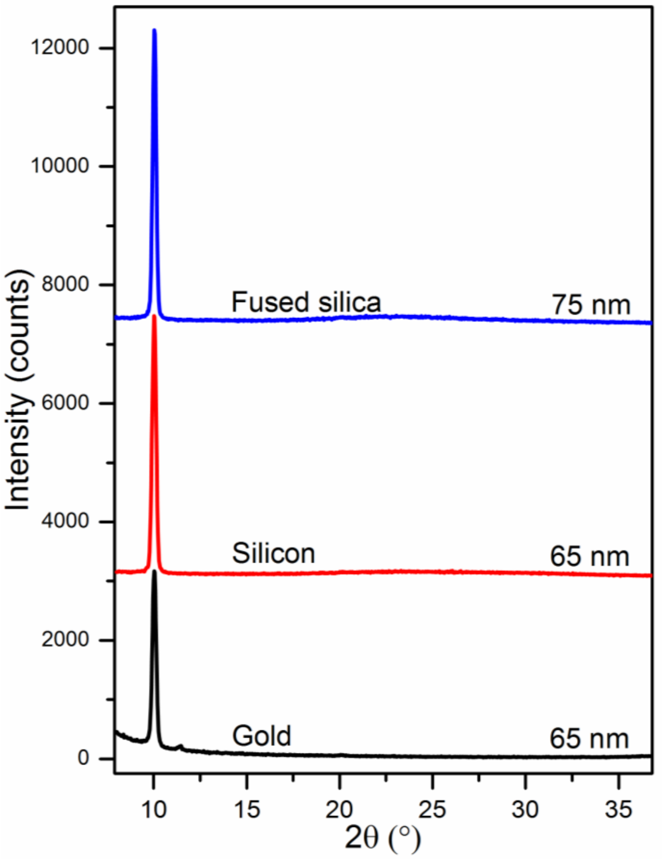

Figure S10. Temperature dependent magnetic measurements for a crystalline film of *ca.* 200 nm thickness, deposited on a paper substrate and rolled-on to increase the quantity of matter analysed. Measurements were done at 2 K/min heating-cooling rate.

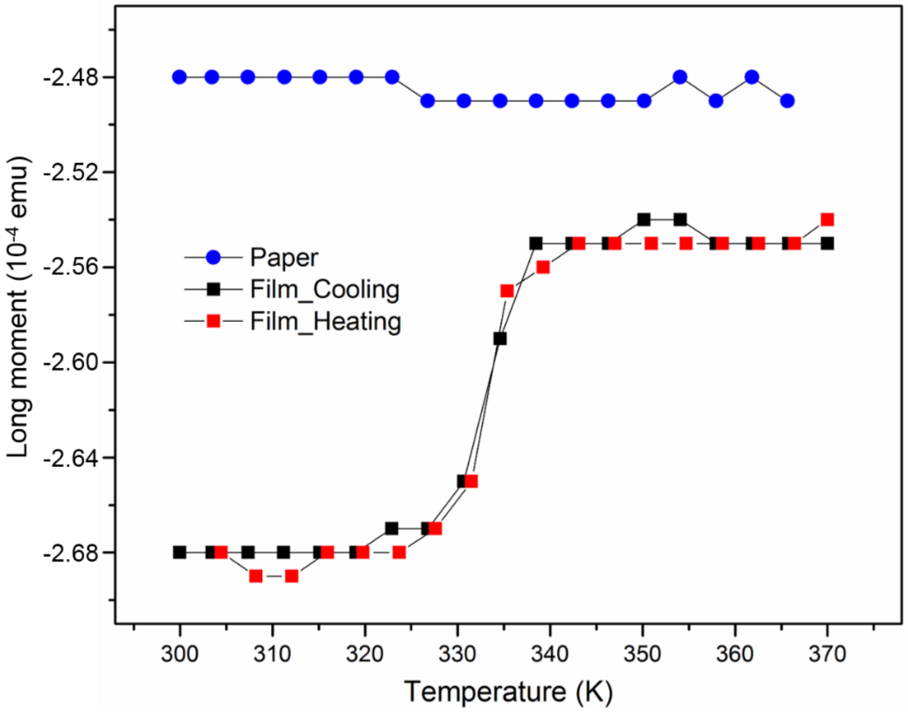

Figure S11. Temperature dependence of the absorbance at 317 nm along four heating-cooling cycles recorded at 1 K/min scan rate for films with thickness of 45 nm (a) and 194 nm (b).

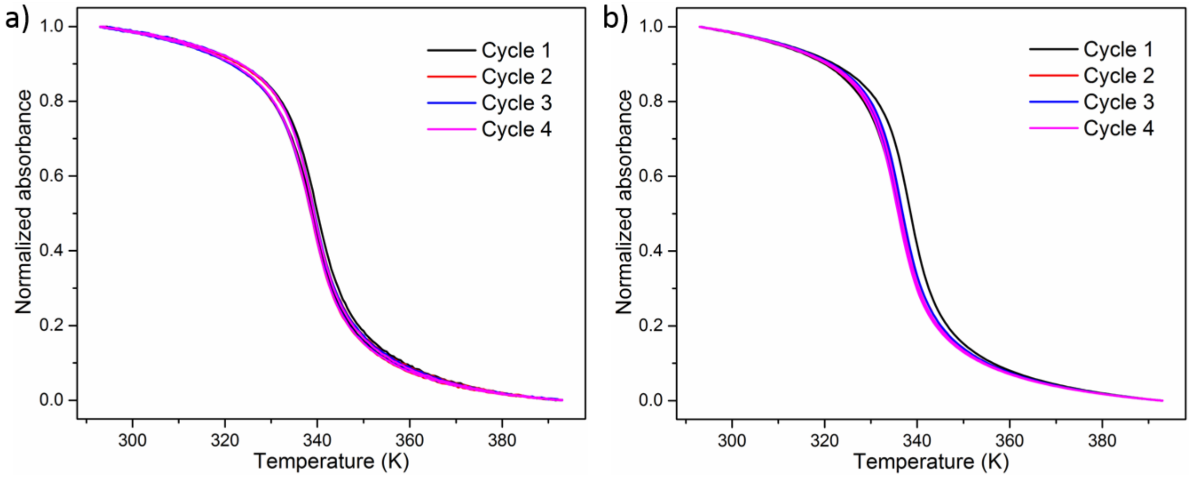

Figure S12. Thermal variation of Raman spectrum of a 194 nm crystalline film on heating.